Local adaptation and dispersal evolution interact to drive population response to climate change

Christopher Weiss-Lehman[1] and Allison K. Shaw[1]

[1]Ecology, Evolution, and Behavior, University of Minnesota

1 Introduction

Climate change is expected to dramatically reshape global biogeographic patterns as some species shift their ranges to track changing environmental conditions (Gonzalez et al., 2010; Peñuelas and Boada, 2003; Hansen et al., 2001; Scholze et al., 2006). These range shifts are generally predicted to proceed upwards in latitude, elevation, or both as average global temperatures continue to rise (Loarie et al., 2009). In fact, contemporary range shifts have already been observed in a wide range of taxa (Chen et al., 2011; Walther et al., 2002; Parmesan and Yohe, 2003; Parmesan, 2006; Parmesan et al., 1999; Perry et al., 2005). Such range shifts present significant challenges to current and future conservation efforts as they can result in both the extinction of populations failing to track a changing climate (Davis and Shaw, 2001; Parmesan, 2006; Zhu et al., 2012; Sekercioglu et al., 2008), and the creation of novel species assemblages as not all species shift their ranges at the same rate or at all (Hobbs et al., 2009; Gilman et al., 2010; Williams and Jackson, 2007), or both. It is therefore crucial to understand the dynamics of such climate-induced range shifts to better inform current and future conservation work.

While the study of range shifts due to climate change is relatively new, important insights can be gained from the related but distinct process of range expansion. Range expansions have been studied for decades, leading to a robust understanding of both the ecological (Skellam, 1951; Hastings et al., 2005) and evolutionary (Shine et al., 2011; Burton et al., 2010; Excoffier et al., 2009; Kubisch et al., 2014) mechanisms responsible for shaping such expansions. For example, while the speed of a

range expansion can be well approximated by a combination of the species' intrinsic growth rate and dispersal ability (Hastings et al., 2005), recent research demonstrates that evolution in both of these traits can have important implications for both the mean and variance of expansion speed through time (Weiss-Lehman et al., 2017; Ochocki and Miller, 2017; Szűcs et al., 2017; Phillips, 2015; Shaw and Kokko, 2015). Since range shifts, like range expansions, have a leading edge of population advance, they are likely to be affected by similar ecological and evolutionary mechanisms as have been shown to drive dynamics in range expansions (Hargreaves and Eckert, 2014). However, while such insights from range expansions are valuable for understanding and predicting dynamics of range shifts, it is important to recognize that these two processes have significant differences as well.

In particular, range expansions and range shifts due to climate change involve fundamentally distinct initial conditions. Range expansions, especially for invasive and reintroduced species, typically begin from the successful establishment and subsequent spread of a small, founding population (Hastings et al., 2005). Such founding populations often represent samples from some larger source population and as such lack any initial spatial population structure. In contrast, range shifts start from entire populations with existing spatial structure within the initially stable range (Hargreaves and Eckert, 2014). Such spatial structure can manifest through local adaptation within the range, the severity of the gradient in population size from the range core to edge, or some combination of the two (Hargreaves and Eckert, 2014; Hargreaves et al., 2015; Henry et al., 2013).

These different aspects of spatial population structure have been shown to dramatically impact the response of populations to climate change. For example, the mechanism responsible for the gradient in population size from core to edge (e.g. declines in birth rates vs. increases in extinction risk) can directly change the probability of extinction a species faces during a climate driven range shift (Henry et al., 2013). A population's risk of extinction during a range shift has also been related to local adaptation within the range. Specifically, a broad environmental niche (i.e. little local adaptation) can decrease a population's ability to track a changing climate if dispersal occurs in a stepping stone manner, allowing some individuals to block dispersal of better adapted genotypes (Atkins and Travis, 2010). Local adaptation also has the potential to interact with dispersal

evolution during climate change, driving increased dispersal probability in an asexual species as genotypes shift to keep pace with their environmental optimum (Hargreaves et al., 2015). However, it is unclear how dispersal evolution and local adaptation might interact in a sexually reproducing species in which dispersal and local adaptation are directly linked via gene flow. For example, evolution of increased dispersal could simultaneously reduce local adaptation within a population due to increased gene flow throughout the range. In fact, long-distance pollen dispersal in flowering plants has been shown to restrict local adaptation and, when pollen dispersal sufficiently outpaces seed dispersal, to lead to ecological niche shifts, rather than spatial range shifts, in response to simulated climate change (Aguilée et al., 2016). Additionally, the distribution of dispersal phenotypes within a population can be influenced by the severity of the gradient at the range edge (Henry et al., 2013; Hargreaves and Eckert, 2014), further complicating the relationship between dispersal evolution and local adaptation during climate-induced range shifts. Evolution during range shifts due to local adaptation and dispersal evolution are both potentially important drivers of range shift dynamics (Van Petegem et al., 2016) and it is therefore important to consider both when predicting the dynamics of populations responding to climate change.

Here, we develop a complex, individual-based model of a sexually reproducing species with two genetically determined traits, one defining an individual's expected dispersal distance and the other determining an individual's environmental niche. Using this model, we simultaneously vary the starkness of the gradient defining the range edge and the potential for local adaptation within the range to ascertain their impact on a population's ability to track a changing climate and how dispersal evolution and local adaptation contribute to the dynamics of the range shift. We additionally compare the dynamics of simulated populations that survived climate change versus those that went extinct to understand the factors contributing to extinction during climate-induced range shifts.

2 Methods

2.1 Overview

2.1.1 Purpose

This model tests an evolving population's ability to track a changing climate under a variety of conditions. Specifically, populations are simulated under different combinations of (1) the starkness of the range boundary and (2) the potential for local adaptation. In all simulations, an individual's expected dispersal distance and environmental niche are defined by an explicit set of quantitative diploid loci subject to mutation, thus allowing both traits to evolve over time. All simulations begin with stable climate conditions for 2000 generations to allow the populations to reach a spatial equilibrium before the onset of climate change. Climate change is then modeled as a constant, directional shift in the location of environmentally suitable habitat (see the *Submodels* section below). Finally, simulations end with another short period of climate stability to assess the population's ability to persist and recover after shifting its range.

2.1.2 State variables and scales

The model simulates a population of male and female individuals characterized by spatial coordinates for their location and by diploid loci for both their expected dispersal distance and environmental niche. Space is modeled as a lattice of discrete patches overlaying a continuous Cartesian coordinate system with a fixed width along the y axis and without bounds on the x axis. To avoid edge effects along the y axis, the model employs wrapping boundaries such that if an individual disperses out of the landscape on one side, it appears at the opposite end of the same column of the landscape. Patches are defined by the location of the patch center in x and y coordinates and a patch width parameter defining the relationship between continuous Cartesian space and the discrete patches used for population dynamics (see the *Submodels* section below).

The environmentally suitable habitat available to a population (i.e. its potential range) is defined by the center of available habitat, the starkness of the decline in suitable habitat away from the center, and the width of suitable habitat (See Figure 1). Environmentally suitable habitat

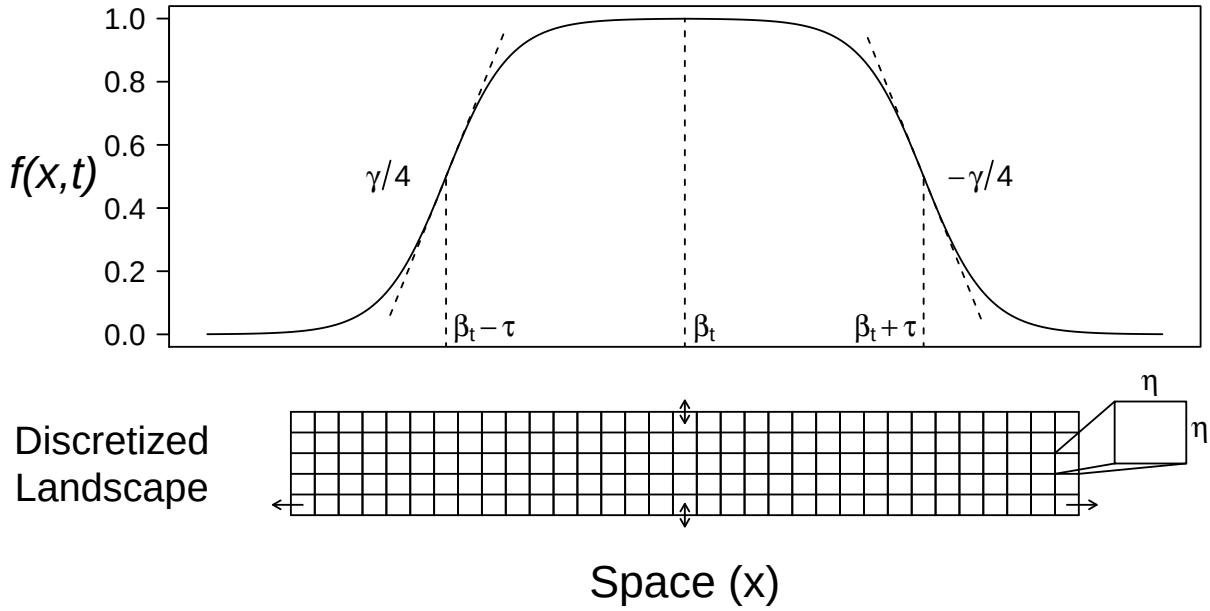

Figure 1: Example of the environmentally suitable habitat available to a population, as defined by $f(x,t)$ in Cartesian space. The parameters of $f(x,t)$ are shown on the figure at significant points along the x axis. The lattice of discrete patches in which population dynamics occur is shown beneath. As described in the *Submodels* section, $f(x,t)$ determines the carrying capacity of the discrete η x η patches. Carrying capacities vary with $f(x,t)$ along the x dimension of the lattice and remain constant within each column along the y dimension. Dispersal is unbounded in the x dimension and implemented with wrapping boundaries in the y dimension.

can shift in space by altering the location of the center of available habitat, which is how climate change is implemented in the model. Further, a gradient in environmental conditions is imposed throughout the landscape to allow for local adaptation via matching of an individual's environmental niche to the local environmental conditions (See *Submodels*). The severity of this gradient can be altered to change the potential for local adaptation (e.g. a shallower gradient will result in more similar environmental conditions throughout the range and therefore reduce the potential for local adaptation).

2.1.3 Process overview and scheduling

Time is also modeled in discrete intervals defining single generations of the population. Within each generation, individuals first disperse from their natal patches according to their dispersal phenotypes (*Submodels*). After dispersal, reproduction occurs according to a stochastic implemen-

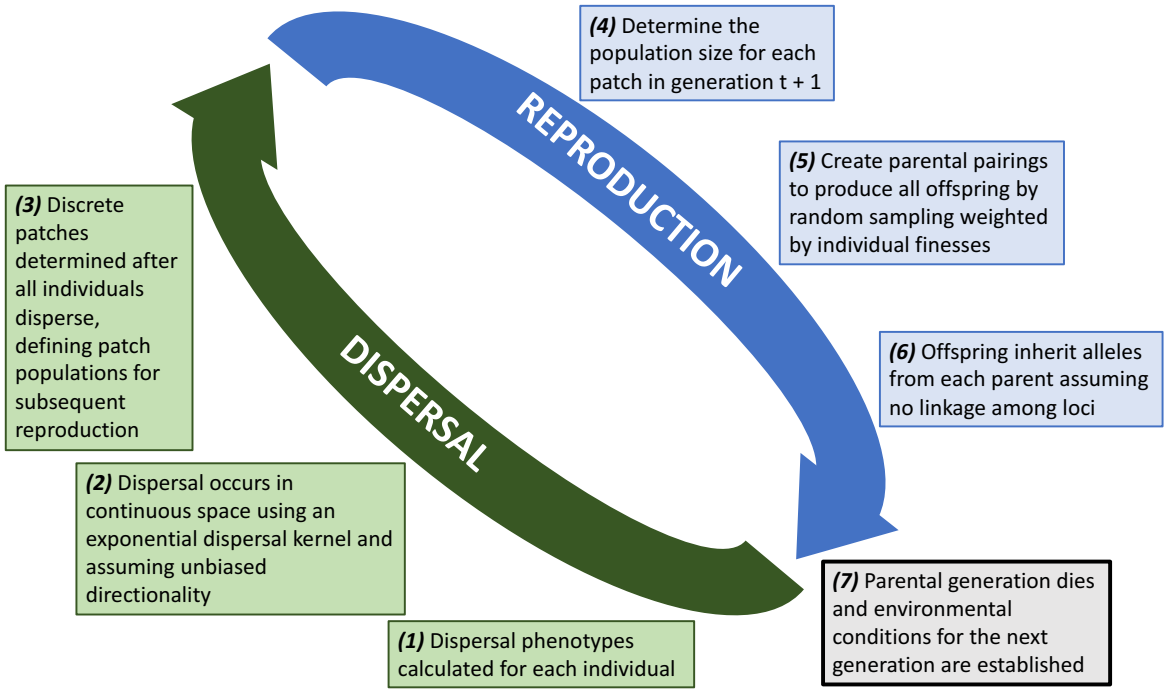

Figure 2: The life cycle of simulated populations is shown divided between events contributing to reproduction and dispersal. Each generation begins with new offspring dispersing according to their phenotype, after which reproduction occurs in local populations defined by the discrete lattice. After reproduction, all parental individuals perish, resulting in discrete, non-overlapping generations.

tation of the classic Ricker model (Ricker, 1954) taking into account the mean fitness of individuals within the patch (*Submodels*). Parental pairs form via random sampling of the local population (with replacement) weighted by individual relative fitness such that individuals with high relative fitness (as determined by the match between their environmental niche and local conditions) are likely to produce multiple offspring while individuals with low relative fitness may not produce any. Individuals inherit one allele from each parent at each loci, assuming independent segregation and a mutation process (*Submodels*). After reproduction, all individuals in the current generation perish and the offspring begin the next generation with dispersal, resulting in discrete, non-overlapping generations.

2.2 Design concepts

2.2.1 Emergence

Emergent phenomena in this model include the spatial equilibrium of population abundances and trait values within the stable range, the demographic dynamics of the shifting population during climate change, and the evolutionary trajectories of both expected dispersal distances and environmental niches during climate change. These are all examined in the context of their impact on the population's ability to keep pace with the changing climate.

2.2.2 Stochasticity

All biological processes in this model are stochastic including realized population growth in each patch, dispersal distances of each individual, and inheritance of loci. Environmental parameters are fixed, however, and the process of climate change (i.e. the movement of environmentally suitable habitat through time) is deterministic. Thus, the model removes the confounding influence of environmental stochasticity to focus on demographic and evolutionary dynamics of range shifts.

2.2.3 Interactions

Individuals in the model interact via mating and density-dependent competition within patches. Other important interactions are the relationship between dispersal evolution and local adaption, particularly in edge populations, and how this relationship impacts a population's ability to avoid extinction and track a changing climate. These interactions are examined in the context of different configurations of the initial, stable range.

2.2.4 Desired output

After each model run, full details of all surviving individuals at the last time point are recorded (spatial coordinates and loci values for both traits). If a population went extinct during the model run, the time of extinction is recorded. Throughout the simulation, certain aggregated values are calculated and recorded for each occupied patch including the population size and the mean and variance of allele values for each trait.

2.3 Details

2.3.1 Initialization

The following parameters are set at the beginning of each simulation and form the initial conditions of the model: the mean and variance for allele values of each trait, population size, location of environmentally suitable habitat, number of generations for the pre-, post-, and during climate change periods of the simulation, and all other necessary parameters for the submodels defined below. Simulated populations are initialized in the center of the range and allowed to spread and equilibrate throughout the range during the period of stable climate conditions. This ensures that the populations reacting to a changing climate truly represent the expected spatial distribution for a given range, rather than the initial parameter values used in the simulation. See Tables 1 & 2 for a full list of parameter values used in the simulations described here.

2.3.2 Submodels

Environmentally suitable habitat Environmentally suitable habitat is determined by the population's carrying capacity as it ranges in space (K_x). The carrying capacity is maximized in the center of the species' range (K_{max}) and declines with increasing distance from the center. Specifically, the carrying capacity at a location x is defined as the product of K_{max} and a function $f(x,t)$, where $f(x,t)$ ranges from 1 in the range center to 0 far away from the center and is defined as follows

$$f(x,t) = \begin{cases} \frac{e^{\gamma(x-\beta_t+\tau)}}{1+e^{\gamma(x-\beta_t+\tau)}} & x \leq \beta_t \\ \frac{e^{-\gamma(x-\beta_t-\tau)}}{1+e^{-\gamma(x-\beta_t-\tau)}} & x > \beta_t \end{cases} \tag{1}$$

where β_t defines the center of the area of suitable habitat at time t, τ sets the width of the range, and γ affects the slope of the function at the range boundaries (See Figure 1). To understand the relationship between γ and the slope of $f(x,t)$ at the range boundary, the partial derivative of

$f(x,t)$ over the spatial dimension can be shown to be

$$f(x,t) = \begin{cases} \frac{\gamma e^{\gamma(x-\beta_t+\tau)}}{(1+e^{\gamma(x-\beta_t+\tau)})^2} & x \leq \beta_t \\ \frac{-\gamma e^{-\gamma(x-\beta_t-\tau)}}{(1+e^{-\gamma(x-\beta_t-\tau)})^2} & x > \beta_t \end{cases} \tag{2}$$

yielding a derivative of $\pm\frac{\gamma}{4}$ at the inflection points on either side of the range center ($x = \beta_t \pm \tau$).

Population dynamics occur within discrete patches, so to calculate a K_x value for a discrete patch from the continuous function $f(x,t)$, we use another parameter defining the spatial scale of each patch (η; See Figure 1). The local carrying capacity of a patch centered on x (K_x) is then calculated as the mean of $f(x,t)$ over the interval of the patch multiplied by K_{max}.

$$K_x = \frac{K_{max}}{\eta} \int_{x-\frac{\eta}{2}}^{x+\frac{\eta}{2}} f(x,t)dx \tag{3}$$

By varying the parameters defining $f(x,t)$, we can change both the total achievable carrying capacity of the population throughout the range (by altering both τ and γ) and the slope at which K_x declines to 0 (by altering γ). Changing the slope affects not only the rate at which K_x declines at the range boundaries (our focus), but it also alters the total achievable carrying capacity of the population. To avoid this confounding factor, we fix the total area under the curve $f(x,t)$. The indefinite integral of $f(x,t)$ can be shown to be

$$\int_{-\infty}^{\infty} f(x,t)dx = \frac{2ln(e^{\gamma\tau}+1)}{\gamma} \tag{4}$$

which can be solved for τ. For a given fixed total area under the curve, an appropriate value of τ can be calculated for each value of γ.

Thus, γ and τ are both fixed within a given simulation and β_t (the location of the center of suitable habitat) is used to simulate climate change. During the periods before and after climate change β_t is constant, but to simulate climate change it varies with time as follows

$$\beta_t = \nu\eta(t-\hat{t}) \tag{5}$$

where ν is the velocity of climate change per generation in terms of discrete patches, η is the spatial scale of each patch, t is the current generation, and $\hat{t}$ is the last generation of stable climatic conditions before the onset of climate change.

Local adaptation To allow an arbitrary degree of local adaptation within the range, the local environmental conditions determining the phenotypic optima ($z_{opt,x}$) are set as follows

$$z_{opt,x} = \lambda(x - \beta_t) \tag{6}$$

where λ defines the potential for local adaptation with values close to 0 resulting in little to no change in phenotypic optimum across the range and values of greater magnitude resulting in large differences in phenotypic optima across the range. Individual relative fitness ($w_{i,x}$) values are then calculated according to the following equation assuming stabilizing selection

$$w_{i,x} = e^{\frac{-(z_i - z_{opt,x})^2}{2\omega^2}} \tag{7}$$

where ω defines the strength of stabilizing selection and z_i is an individual's environmental niche (Lande, 1976). Thus, an individual's realized fitness will be higher the closer its environmental niche ($z_{[}i]$) is to the local environmental conditions of the patch it occupies ($z_{opt,x}$). All loci are assumed to contribute additively to an individual's environmental niche value with no dominance or epistasis, meaning an individual's phenotype is simply the sum of the individual's allele values.

Population dynamics Population growth within each patch is modeled with a stochastic implementation of the classic Ricker model (Ricker, 1954; Melbourne and Hastings, 2008). To account for fitness effects on population growth, expected population growth is scaled by the mean relative fitness of individuals within the patch ($\bar{w_x}$). The expected number of new offspring in patch x at time $t + 1$ is then given by

$$\hat{N}_{t+1,x} = \bar{w_x} F_{t,x} \frac{R}{\psi} e^{\frac{-RN_{t,x}}{K_x}} \tag{8}$$

where $F_{t,x}$ is the number of females in patch x at time t, R is the intrinsic growth rate for the population, ψ is the expected sex ratio of the population, $N_{t,x}$ is the number of individuals (males and females) in patch x at time t, and K_x is the local carrying capacity based on the environmental conditions. To incorporate demographic stochasticity, the realized number of offspring for each patch is then drawn from a Poisson distribution.

$$N_{t+1,x} \sim Poisson(\hat{N}_{t+1,x}) \tag{9}$$

Parentage of the offspring is then assigned by random sampling of the local male and female population (i.e. polygynandrous mating). The sampling is weighted by individual fitness and occurs with replacement so highly fit individuals are likely to have multiple offspring while low fitness individuals may not have any. Each offspring inherits one allele per locus from each parent, assuming no linkage among loci. After reproduction, all members of the previous generation die and the offspring disperse to begin the next generation.

Mutation Inherited alleles are subject to mutation such that some offspring might not inherit identical copies of certain alleles from their parents. The mutation process is defined by two parameters for each trait T: the diploid mutation rate (U^T) and the mutational variance (V_m^T). Using these parameters along with the number of loci defining trait T (L^T), the per locus probability of a mutation is

$$\frac{U^T}{2L^T} \tag{10}$$

Mutational effects are drawn from a normal distribution with mean 0 and a standard deviation of

$$\sqrt{V_m^T U^T} \tag{11}$$

By defining the mutation process in this manner rather than setting a probability of mutation and mutational effect directly, similar mutational dynamics can be imposed regardless of the number of loci used in the simulation.

Dispersal Finally, individuals disperse according to an exponential dispersal kernel defined by each individual's dispersal phenotype. An individual's dispersal phenotype is the expected dispersal distance and is given by

$$d_i = \frac{D\eta e^{\rho \Sigma L^D}}{1 + e^{\rho \Sigma L^D}} \tag{12}$$

where D is the maximum expected dispersal distance in terms of discrete patches, η is the spatial scale of discrete patches, ρ is a constant determining the slope of the transition between 0 and D, and the summation is taken across all alleles contributing to dispersal. Thus, as with fitness, loci are assumed to contribute additively with no dominance or epistasis. The expected dispersal distance, d_i is then used to draw a realized distance from an exponential dispersal kernel. The direction of dispersal is drawn from a uniform distribution bounded by 0 and 2π. If a dispersal trajectory takes an individual outside the bounds of the landscape in the y axis, the individual reappears at the same x coordinate but the opposite end of the y axis, thus wrapping the top and bottom edges of the landscape to avoid edge effects. Dispersal occurs from the center of each patch and the individual's new patch is then determined according to its location in the overlaid grid of η x η patches (see Figure 1).

2.4 Simulation experiments

Most of the parameters described above were held constant over all simulations (Table 1), but we varied certain parameter values to explore the interacting roles of local adaptation and the starkness of the gradient in environmentally suitable habitat at the range edge (Table 2). Specifically, we considered a factorial combination of no, low, and high potential for local adaptation with shallow, moderate, and stark gradients in habitat quality at the range edge for a total of 9 different scenarios, each explored with 200 simulations. Each simulation ran for 2150 generations with stable climate conditions for the first 2000, followed by 100 generations of climate change and a final 50 generations of stable conditions. Figure 3 shows an example of a single simulation undergoing climate change. All simulations were performed in R version 3.4.4 (Team, 2000) and the code is available at `https://github.com/tpweiss06/ShiftingSlopes`. Additionally, we explored the role of the rate of climate change on the dynamics of range shifts in these different scenarios, examining both slower and faster

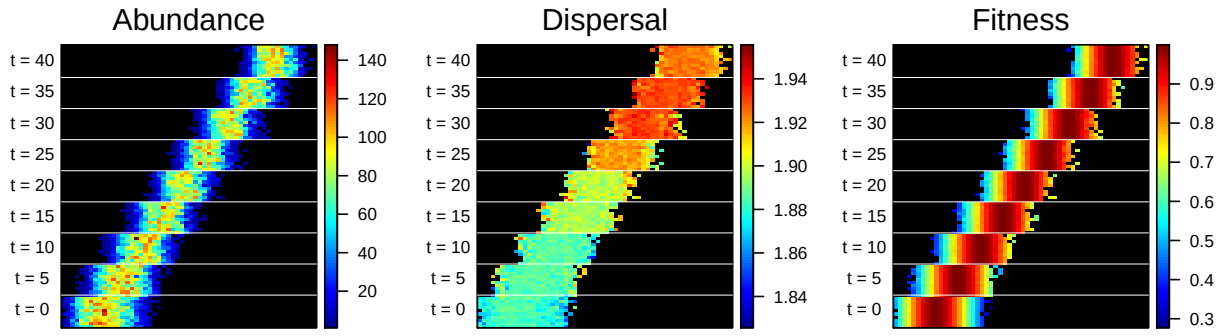

Figure 3: A single example of a simulation with a high potential for local adaptation and a moderate gradient at the range edge. Information on the abundance, dispersal, and fitness of each patch in the population is shown for time periods beginning with the last generation of stable climate conditions ($t = 0$) to 40 generations after the start of climate change ($t = 40$). For the dispersal trait, individual phenotypes were calculated according to equation 12 and the local population mean was calculated for each patch. The log transformed local means are shown on the graph. Average patch fitness was calculated based on the mean local environmental niche and the optimal niche value for that location according to equation 7.

speeds of climate change (see *Appendix*).

3 Results

3.1 Extinction probability

To assess the joint impact of the potential for local adaptation and the severity of the environmental gradient defining the range edge on the probability of extinction during climate change, we calculated the proportion of simulated populations to go extinct through time for the 100 generations of simulated climate change (Figure 4). Increases in both the potential for local adaptation and the severity of the gradient at the range edge resulted in increased probabilities of extinction through time. However, increased potential for local adaptation seemed to drive larger changes in extinction probabilities than increases in the severity of habitat gradients, at least over the parameter values examined here. Similar patterns were observed for both slower and faster speeds of climate change. As expected, slower speeds of climate change resulted in reduced probabilities of extinction while faster speeds of climate change increased extinction probabilities in all scenarios, but the potential

Parameter	Description	Value
N_1	Initial population size (seeded across multiple patches) when beginning the simulations	2500
β_1	Center of environmentally suitable habitat before climate change	0
η	Spatial dimensions of habitat patches in continuous space	50
y_{max}	Number of patches the discrete lattice extends in the y direction	10
$\hat{t}$	Last time point of stable climate conditions	2000
t_Δ	Duration of climate change	100
t_{max}	Total number of time points in the simulation	2150
R	Intrinsic growth rate of the population	2
K_{max}	Maximum achievable carrying capacity in the range	100
ψ	Expected sex ratio in the population	0.5
D	Maximum achievable dispersal phenotype	1000
ρ	Determines the slope of the transition in dispersal phenotypes from 0 to D	0.5
ω	Defines the strength of stabilizing selection on fitness traits	3
U^T	Diploid mutation rate for each trait	0.02 for each trait
V_m^T	Mutational variance for each trait	0.0004 for each trait
L^T	The number of diploid loci defining each trait	5 for each trait
μ_1^f	The initial mean allele value for the environmental niche trait	0
μ_1^d	The initial mean allele value for the dispersal trait	-1
σ_1^f	The initial standard deviation of allele values for the environmental niche trait	0.025
σ_1^d	The initial standard deviation of allele values for the dispersal trait	1

Table 1: Simulation parameters held constant across all scenarios presented here.

Habitat gradient at range edge	Potential for local adaptation	γ	τ	λ
Shallow	None	0.0025	250	0
	Low	0.0025	250	0.004
	High	0.0025	250	0.008
Moderate	None	0.025	421.479	0
	Low	0.025	421.479	0.004
	High	0.025	421.479	0.008
Stark	None	0.25	421.48	0
	Low	0.25	421.48	0.004
	High	0.25	421.48	0.008

Table 2: Descriptions and parameter values for the 9 different scenarios examined here.

for local adaptation and the severity of the environmental gradient at the range edge caused similar increases in extinction probability at all speeds of climate change (see Appendix).

3.2 Initial conditions

Examining those simulations that survived climate change and comparing them to the simulated populations that went extinct revealed key differences driving extinction dynamics during climate change. Primarily, the simulations that survived were largely composed of higher dispersal phenotypes at the beginning of climate change compared to the simulations that went extinct (Fig. 5), suggesting an important role for the initial distribution of dispersal traits in populations responding to climate change. In fact, a threshold seems to divide populations that ultimately survived climate change from those that went extinct at roughly a mean dispersal phenotype of 100. This corresponds to a roughly 10% chance of an individual moving a single patch in the x dimension, which would be sufficient to keep the same relative location in the range during climate change in our simulations. Examining simulations with different speeds of climate change reveals that this threshold varies with the speed of climate change, but similarly divides extinct from surviving populations (see Appendix).

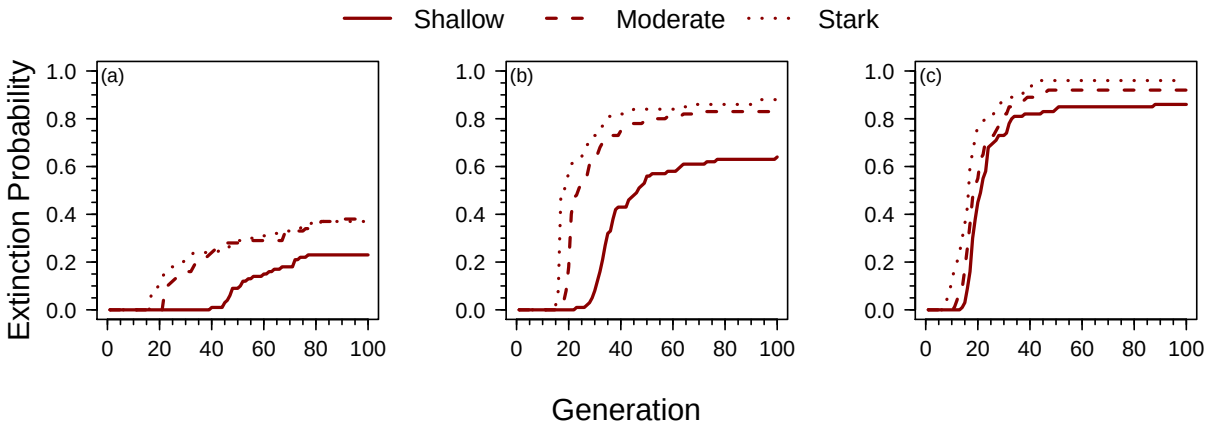

Figure 4: The cumulative probability of extinction during climate change in experimental scenarios. The probabilities of extinction for simulated populations with no potential for local adaptation are shown in panel (a). The probabilities of extinction for simulated populations with low and high potential for local adaptation are shown in panels (b) and (c) respectively. In each panel populations characterized by a shallow, moderate, or stark gradient at the range edge are shown with solid, dashed, and dotted lines respectively as shown in the legend. Cumulative probabilities of extinction were calculated as the proportion of simulated populations to be extinct through time.

Additionally, the simulations that survived climate change tended to be characterized by reduced fitness at the range margins compared to simulated populations that went extinct (Fig. 6). This pattern was most evident in the simulations with (1) a gradual environmental gradient at the range edge and (2) high potential for local adaptation. It was not present in simulations with no potential for local adaptation. As the simulations that survived climate change were also characterized by heightened dispersal (Fig. 5), the observed reduction in average patch fitness at the margins is likely due to increased gene flow from the range core hampering the abilities of these edge populations to adapt to local conditions.

3.3 Dispersal evolution

To quantify dispersal evolution due to climate change, we calculated the change in the mean dispersal phenotypes of individual patches from the beginning of the period to climate change to the end. For patches that were unoccupied by the end of the period of climate change due to population extinction, we used the last generation in which the population had at least 10

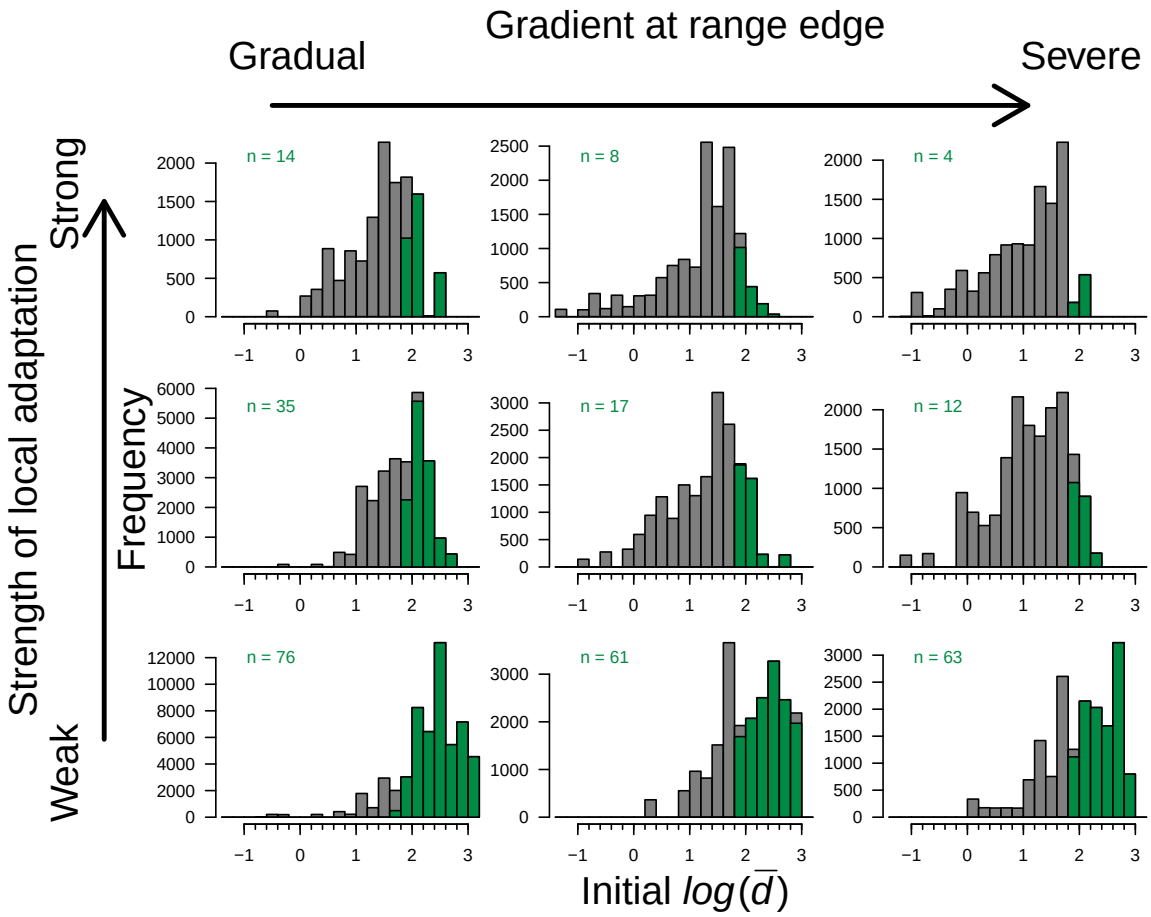

Figure 5: Histograms of the log transformed mean dispersal phenotypes in each patch after 2000 generations of stable climate conditions. On each histogram, the values associated with populations surviving climate change are highlighted in green and the total number of simulated populations to survive climate change is indicated in the top left corner. Each histogram represents one of the 9 experimental scenarios examined here, with potential for local adaptation increasing from none to high from top to bottom and the severity of the gradient at the range edge increasing from gradual to severe from left to right as indicated on the figure.

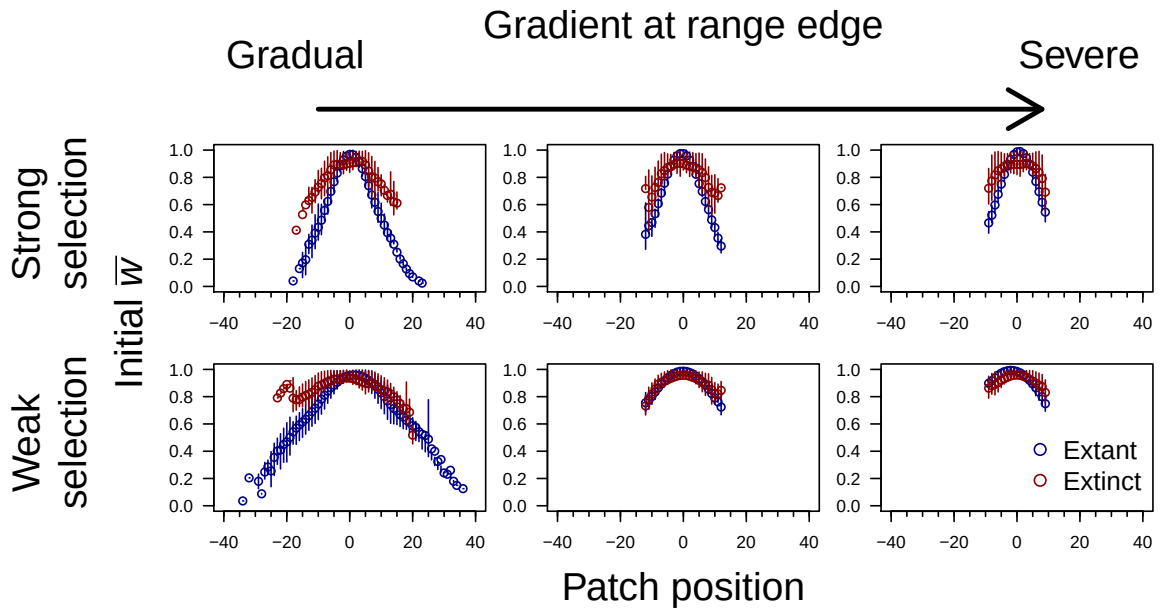

Figure 6: Mean patch level fitness along the x dimensions of the landscape after 2000 generations of stable climate conditions for both extant (those populations that ultimately survived climate change) and extinct populations. Points represent the mean value across simulations and error bars are interquartile ranges. The experimental scenario corresponding to each panel is shown on the graph and simulations with no potential for local adaptation are not shown as, by definition, patch fitness does not vary spatially.

individuals as the end point to calculate change in mean dispersal phenotype. For this analysis, we defined individual patches by their relative location within the range rather than with their fixed spatial coordinates. In this way, we calculated change in mean dispersal phenotype for populations consistently occupying the same position relative to the range center (e.g. leading edge vs. core populations). Changes in mean dispersal phenotype were calculated by subtracting the initial mean dispersal phenotype from the value at the end of climate change (or at the last generation of at least 10 individuals occupying the patch in the case of population extinctions) so that positive values indicate an increase in the mean dispersal phenotype.

Dispersal evolved in all simulated populations throughout the period of climate change. However, there was no substantial difference in the evolutionary trajectories of dispersal in populations that successfully tracked climate change versus those that went extinct (Fig. 7). Additionally, contrary to expectations, range shifts did not result in the evolution of significantly increased dispersal capabilities. Rather, simulated populations underwent both increases and decreases in average dispersal capability, though the scale of changes was small compared to the distinction seen between extant and extinct populations in initial dispersal phenotypes (Figs. 5 & 7). Essentially, the magnitude of dispersal evolution possible in the time scale of simulated climate change did not seem to be able to rescue populations starting from initial conditions characterized by lower dispersal capabilities.

4 Discussion

Range shifts due to climate change represent a global threat to biodiversity and much recent research has focused on exploring the underlying ecological and evolutionary dynamics of such range shifts to inform conservation efforts. While previous models have focused on ecological dynamics (CITATIONS), evolution in dispersal only (CITATIONS), and relatively simple genetic scenarios (e.g. single-locus haploid genetics in asexual populations) (CITATIONS), we developed an individual-based model to explore the eco-evolutionary dynamics of climate induced-range shifts in sexually reproducing, diploid populations with both dispersal and environmental niche traits defined by multiple loci. Using this model, we demonstrated the role of spatial population structure, in the

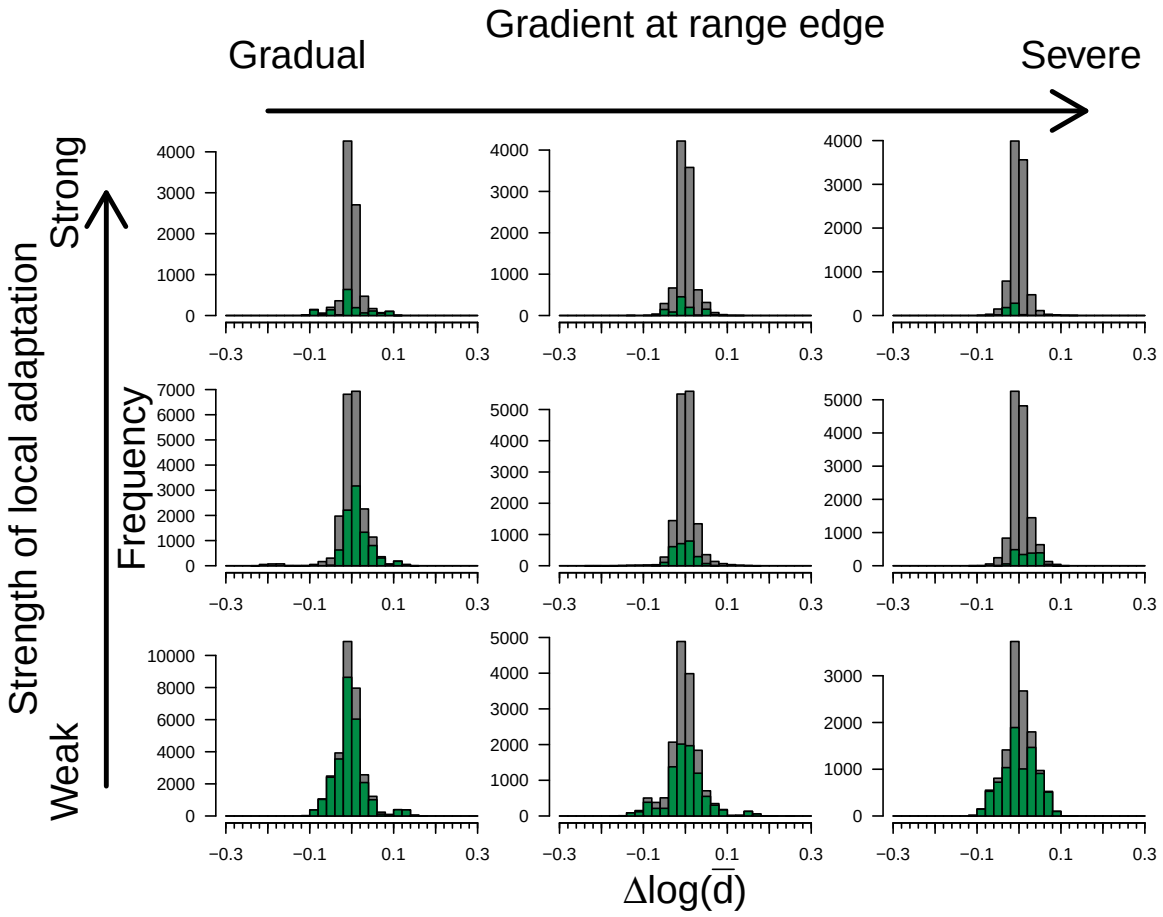

Figure 7: Histograms of the change in the log transformed mean dispersal phenotypes in each patch from the beginning of the period of climate change to the end. Positive values indicate an increase in average dispersal ability in the patch. Each patch was defined by its location relative to the range center (β_t) so changes in dispersal correspond to relative (e.g. leading and trailing edge patches), as opposed to absolute (i.e. fixed spatial coordinates), locations in the range. For those simulated populations that went extinct during climate change, we calculated the change in dispersal phenotype using the last time point with at least 10 individuals in the patch as described in the text. The values associated with populations that survived climate change are highlighted in green on the graphs. Each histogram represents one of the 9 experimental scenarios examined here, denoted by the text and arrows on the figure.

form of local adaptation and the environmental gradient defining the range edge, in determining extinction risk for range shifting populations via impacts on the initial distribution of dispersal phenotypes and environmental niche values.

Both the potential for local adaptation and the severity of the environmental gradient at the range edges significantly impacted the probability of extinction for populations during climate change (Fig. 4) with the potential for local adaptation seeming to cause more dramatic increases. The parameters defining both of these range attributes were varied widely (the potential for local adaptation doubled from the low to high scenario and the parameter defining the severity of the environmental gradient was increased by a factor of 100 from shallow to stark gradients; Table 2), suggesting that potential for local adaptation may be the stronger driver of extinction risk during climate-induced range shifts across a wide region of parameter space. While overall extinction probability changed as expected with different speeds of climate change, the effects of increased potential for local adaptation and increased severity of the environmental gradient at the range edges on extinction probability remained the same (see Appendix).

These extinction dynamics seemed to manifest via the distribution of dispersal phenotypes that evolved in response to different aspects of spatial population structure. Simulated populations that survived climate change all began the period of climate change with populations defined by heightened dispersal phenotypes (Fig. 5). In particular, the surviving populations all began climate change with populations defined by dispersal phenotypes at or above the threshold necessary for about 10% of the population to keep pace with the changing climate. In scenarios with higher potential for local adaptation and more severe gradients at the range edge, simulated populations were less likely to have such high dispersal phenotypes due to selection against high dispersal distances due to local adaptation (CITATIONS) and the risk of dispersing beyond the boundary of suitable habitat (CITATION). As a result, populations in those scenarios faced a greater risk of extinction during climate change. This threshold value of dispersal phenotypes changed accordingly with the speed of climate change, accounting for the resultant changes in extinction probability under the different scenarios (see Appendix).

While high dispersal phenotypes prior to climate change allowed populations to survive, it had

the additional effect of reducing average fitness at the range margins in scenarios with the potential for local adaptation (Fig. 6). In the model, populations at the range margins tended to be lower abundance than populations in the range core, thus increasing their susceptibility to gene flow from the core (CITATION). Thus, when populations were defined by high dispersal phenotypes prior to climate change, it reduced fitness at the range margin due to gene flow preventing adaptation to local conditions. As a result, the populations most likely to survive climate change were, counter-intuitively, also those characterized by lower fitness prior to the start of climate change. While not all populations are characterized by small populations at the range edges (CITATION), and thus are unlikely to be equally susceptible to the influence of gene flow from the core, our results suggest that populations exhibiting high levels of local adaptation within their stable range are likely to be at greater risk of extinction during periods of climate change.

Previous research has suggested that evolution of increased dispersal ability during climate change may be able to rescue populations that would otherwise be unable to keep pace with shifting environmental conditions (CITATIONS). Our results suggest this is not always the case, and in fact may only be possible under certain, relatively narrow conditions. Models finding that dispersal evolution may rescue populations during climate change have typically used relatively simple genetic frameworks to model dispersal, including haploid (CITATION) and single-locus models (CITATION). Such simplified genetic frameworks can increase the potential for evolutionary change by, for example, increasing the effect of individual mutations (CITATION). Additionally, many previous models of climate-induced range shifts have used asexual reproduction, which can also increase the potential for evolutionary change by allowing for near complete fidelity of trait values passed from parent to offspring (CITATION). The negligible role played by dispersal evolution in our model (Fig. 7) suggests that when such simplifying assumptions are relaxed the potential for population rescue via evolution of heightened dispersal is greatly reduced, thus increasing the role of the initial spatial population structure within the range in determining a population's fate under climate change.

4.1 Conclusion

Understanding the various ecological and evolutionary drivers of climate-induced range shifts is crucial to current and future conservation efforts. In particular, we need to better understand how these various mechanisms combine to shape the extinction probabilities of populations undergoing range shifts, which, in turn, will allow more focused interventions. Our results suggest that initial spatial population structure, as determined by local adaptation and the environmental gradient at the range edge, has the potential to dramatically alter the extinction probability faced by species responding to climate change. Further, in contrast to other studies assuming more simplified breeding and genetic structure, we find very little role for the evolution of heightened dispersal abilities to rescue a population composed of low-dispersing individuals. Future work should continue to examine the interplay between initial conditions in range shifts and the potential for evolutionary rescue. As climate change continues to accelerate (CITATION), it is imperative to not only identify those factors leading to increased extinction risk in range shifting populations, but also to develop meaningful conservation strategies to mitigate such increased risk.

References

Aguilée, R., G. Raoul, F. Rousset, and O. Ronce. 2016. Pollen dispersal slows geographical range shift and accelerates ecological niche shift under climate change. Proceedings of the National Academy of Sciences 113:E5741–E5748.

Atkins, K., and J. Travis. 2010. Local adaptation and the evolution of species' ranges under climate change. Journal of Theoretical Biology 266:449–457.

Burton, O. J., B. L. Phillips, and J. M. Travis. 2010. Trade-offs and the evolution of life-histories during range expansion. Ecology Letters 13:1210–1220.

Chen, I.-C., J. K. Hill, R. Ohlemüller, D. B. Roy, and C. D. Thomas. 2011. Rapid range shifts of species associated with high levels of climate warming. Science 333:1024–1026.

392 Davis, M. B., and R. G. Shaw. 2001. Range shifts and adaptive responses to quaternary climate
393 change. Science 292:673–679.

394 Excoffier, L., M. Foll, and R. J. Petit. 2009. Genetic consequences of range expansions. Annual
395 Review of Ecology, Evolution, and Systematics 40:481–501.

396 Gilman, S. E., M. C. Urban, J. Tewksbury, G. W. Gilchrist, and R. D. Holt. 2010. A framework
397 for community interactions under climate change. Trends in Ecology & Evolution 25:325–331.

398 Gonzalez, P., R. P. Neilson, J. M. Lenihan, and R. J. Drapek. 2010. Global patterns in the
399 vulnerability of ecosystems to vegetation shifts due to climate change. Global Ecology and
400 Biogeography 19:755–768.

401 Hansen, A. J., R. P. Neilson, V. H. Dale, C. H. Flather, L. R. Iverson, D. J. Currie, S. Shafer,
402 R. Cook, and P. J. Bartlein. 2001. Global change in forests: Responses of species, communities,
403 and biomes: Interactions between climate change and land use are projected to cause large shifts
404 in biodiversity. AIBS Bulletin 51:765–779.

405 Hargreaves, A., S. Bailey, and R. A. Laird. 2015. Fitness declines towards range limits and local
406 adaptation to climate affect dispersal evolution during climate-induced range shifts. Journal of
407 Evolutionary Biology 28:1489–1501.

408 Hargreaves, A. L., and C. G. Eckert. 2014. Evolution of dispersal and mating systems along
409 geographic gradients: implications for shifting ranges. Functional Ecology 28:5–21.

410 Hastings, A., K. Cuddington, K. F. Davies, C. J. Dugaw, S. Elmendorf, A. Freestone, S. Harrison,
411 M. Holland, J. Lambrinos, U. Malvadkar, et al. 2005. The spatial spread of invasions: new
412 developments in theory and evidence. Ecology Letters 8:91–101.

413 Henry, R. C., G. Bocedi, and J. M. Travis. 2013. Eco-evolutionary dynamics of range shifts: elastic
414 margins and critical thresholds. Journal of Theoretical Biology 321:1–7.

415 Hobbs, R. J., E. Higgs, and J. A. Harris. 2009. Novel ecosystems: implications for conservation
416 and restoration. Trends in Ecology & Evolution 24:599–605.

417 Kubisch, A., R. D. Holt, H.-J. Poethke, and E. A. Fronhofer. 2014. Where am i and why? synthe-
418 sizing range biology and the eco-evolutionary dynamics of dispersal. Oikos 123:5–22.

419 Lande, R. 1976. Natural selection and random genetic drift in phenotypic evolution. Evolution
420 30:314–334.

421 Loarie, S. R., P. B. Duffy, H. Hamilton, G. P. Asner, C. B. Field, and D. D. Ackerly. 2009. The
422 velocity of climate change. Nature 462:1052.

423 Melbourne, B. A., and A. Hastings. 2008. Extinction risk depends strongly on factors contributing
424 to stochasticity. Nature 454:100.

425 Ochocki, B. M., and T. E. Miller. 2017. Rapid evolution of dispersal ability makes biological
426 invasions faster and more variable. Nature Communications 8:14315.

427 Parmesan, C. 2006. Ecological and evolutionary responses to recent climate change. Annual Review
428 of Ecology, Evolution, and Systematics 37:637–669.

429 Parmesan, C., N. Ryrholm, C. Stefanescu, J. K. Hill, C. D. Thomas, H. Descimon, B. Huntley,
430 L. Kaila, J. Kullberg, T. Tammaru, et al. 1999. Poleward shifts in geographical ranges of butterfly
431 species associated with regional warming. Nature 399:579.

432 Parmesan, C., and G. Yohe. 2003. A globally coherent fingerprint of climate change impacts across
433 natural systems. Nature 421:37.

434 Peñuelas, J., and M. Boada. 2003. A global change-induced biome shift in the montseny mountains
435 (ne spain). Global Change Biology 9:131–140.

436 Perry, A. L., P. J. Low, J. R. Ellis, and J. D. Reynolds. 2005. Climate change and distribution
437 shifts in marine fishes. Science 308:1912–1915.

438 Phillips, B. L. 2015. Evolutionary processes make invasion speed difficult to predict. Biological
439 Invasions 17:1949–1960.

440 Ricker, W. E. 1954. Stock and recruitment. Journal of the Fisheries Board of Canada 11:559–623.

441 Scholze, M., W. Knorr, N. W. Arnell, and I. C. Prentice. 2006. A climate-change risk analysis for
442 world ecosystems. Proceedings of the National Academy of Sciences 103:13116–13120.

443 Sekercioglu, C. H., S. H. Schneider, J. P. Fay, and S. R. Loarie. 2008. Climate change, elevational
444 range shifts, and bird extinctions. Conservation Biology 22:140–150.

445 Shaw, A. K., and H. Kokko. 2015. Dispersal evolution in the presence of allee effects can speed up
446 or slow down invasions. The American Naturalist 185:631–639.

447 Shine, R., G. P. Brown, and B. L. Phillips. 2011. An evolutionary process that assembles phenotypes
448 through space rather than through time. Proceedings of the National Academy of Sciences
449 108:5708–5711.

450 Skellam, J. G. 1951. Random dispersal in theoretical populations. Biometrika 38:196–218.

451 Szűcs, M., M. Vahsen, B. Melbourne, C. Hoover, C. Weiss-Lehman, and R. Hufbauer. 2017. Rapid
452 adaptive evolution in novel environments acts as an architect of population range expansion.
453 Proceedings of the National Academy of Sciences 114:13501–13506.

454 Team, R. C. 2000. R language definition. Vienna, Austria: R Foundation for Statistical Computing.
455 .

456 Van Petegem, K. H., J. Boeye, R. Stoks, and D. Bonte. 2016. Spatial selection and local adaptation
457 jointly shape life-history evolution during range expansion. The American Naturalist 188:485–
458 498.

459 Walther, G.-R., E. Post, P. Convey, A. Menzel, C. Parmesan, T. J. Beebee, J.-M. Fromentin,
460 O. Hoegh-Guldberg, and F. Bairlein. 2002. Ecological responses to recent climate change. Nature
461 416:389.

462 Weiss-Lehman, C., R. A. Hufbauer, and B. A. Melbourne. 2017. Rapid trait evolution drives
463 increased speed and variance in experimental range expansions. Nature Communications 8:14303.

464 Williams, J. W., and S. T. Jackson. 2007. Novel climates, no-analog communities, and ecological
465 surprises. Frontiers in Ecology and the Environment 5:475–482.

466 Zhu, K., C. W. Woodall, and J. S. Clark. 2012. Failure to migrate: lack of tree range expansion in
467 response to climate change. Global Change Biology 18:1042–1052.